View metadata, citation and similar papers at core.ac.uk

brought to you by CORE

provided by CURVE/open

Establishing isothermal contact at a known temperature under thermal equilibrium in elevated temperature instrumented indentation testing

Hou, X, Alvarez, CLM & Jennett, NM

Author post-print (accepted) deposited by Coventry University's Repository

Original citation & hyperlink:
Hou, X, Alvarez, CLM & Jennett, NM 2017, 'Establishing isothermal contact at a known temperature under thermal equilibrium in elevated temperature instrumented indentation testing' *Measurement Science and Technology*, vol 28, no. 2, 025016
https://dx.doi.org/10.1088/1361-6501/aa533d

DOI 10.1088/1361-6501/aa533d
ISSN 0957-0233
ESSN 1361-6501

Publisher: IOP Publishing

Copyright © and Moral Rights are retained by the author(s) and/ or other copyright owners. A copy can be downloaded for personal non-commercial research or study, without prior permission or charge. This item cannot be reproduced or quoted extensively from without first obtaining permission in writing from the copyright holder(s). The content must not be changed in any way or sold commercially in any format or medium without the formal permission of the copyright holders.

This document is the author's post-print version, incorporating any revisions agreed during the peer-review process. Some differences between the published version and this version may remain and you are advised to consult the published version if you wish to cite from it.

Establishing isothermal contact at a known temperature under thermal equilibrium in elevated temperature instrumented indentation testing

X.D. Hou[1], C.L.M. Alvarez[2] and N.M. Jennett[3]

[1] National Physical Laboratory, Teddington TW11 0LW, UK
[2] Asociación de Investigación Metalúrgica del Noroeste, Pontevedra, Spain
[3] Coventry University, Coventry, CV1 5FB, UK

Abstract

Instrumented indentation testing (IIT) at elevated temperatures has proved to be a useful tool to study plastic and elastic deformation and understand the performance of material components at (or nearer to) the actual temperatures experienced in-service. The value of elevated temperature IIT data, however, depends on the ability not only to achieve a stable, isothermal indentation contact at thermal equilibrium when taking data, but to be able to assign a valid temperature to that contact (and so to the data). The most common method found in the current literature is to use the calculated thermal drift rate as an indicator, but this approach has never been properly validated. This study proves that using the thermal drift rate to determine isothermal contact may lead to large errors in the determination of the real contact temperature. Instead, a more sensitive and validated method is demonstrated, based upon using the indenter tip and the tip heater control thermocouple as a reproducible and calibrated contact temperature sensor. A simple calibration procedure is described, along with step by step guidance to establish an isothermal contact at a known temperature under thermal equilibrium when conducting elevated temperature IIT experiments.

Keywords: nano-indentation; elevated temperature; thermal equilibrium; isothermal contact

1. Introduction

Instrumented indentation testing (IIT) at elevated temperatures has proven to be a useful tool to obtain mechanical properties of material components representative of in-service conditions [1,2,3,4,5,6]. As a result, in recent years, an increasing number of studies have been reported focussing both on achieving a better understanding of the thermal mechanisms behind the technique, and on developing the equipment required to extend instrument capabilities further – mainly targeting increasing the achievable temperatures, preventing oxidation phenomena and developing stable high-temperature indenters [7].

The calibration of IIT systems is clearly outlined in ISO 14577 including force, displacement, indenter area function and frame compliance [8]. When operating at elevated temperatures, however, the significant heat input to the IIT system invalidates and changes the calibrations of the system obtained at ambient temperature [9]. In addition to the validation of the system calibration, the key challenge is to be able to control and accurately assign the correct temperature to the contact point. There is a growing body of literature describing the importance of achieving thermal equilibrium, and different thermal management approaches have been proposed. For IIT systems able only to heat the sample (with a passively heated indenter), a long stabilisation period is recommended with the indenter held in contact with the sample until the thermal drift is minimised [3]. Of great advantage is, therefore, to heat the sample and indenter independently to: shorten stabilization time, lower the thermal gradient and reduce restrictions on the sample thermal conductivity [10]. The current state of art technology in thermal drift and thermal gradient management is described in a recent review by Wheeler et al [11]. It was clearly demonstrated in this review that typical current practice uses the minimisation of the measured thermal drift rate as an indicator of a thermal equilibrium state. Whilst it is practically convenient to use an indentation thermal drift value, the measured displacement drift rate is always a sum of all occurring displacement drift rates, which may be of opposite signs. This includes: stage drift, combined thermal expansion of the instrument + sample + tip, as well as transducer and electronic drift and material creep under load (especially when indenting soft materials or materials that become soft when heated). There is always a possibility that the measured net thermal drift is very small only as a result of compensating contributions from different components.

It is also important to distinguish thermal equilibrium from isothermal contact. Thermal equilibrium can exist whenever the heat flow is stabilised, however this can occur with either high or low thermal gradients in the instrument, sample and/or across the contact. It is important to know the thermal gradients in order to assign and accurate contact temperature. This is because the contact temperature can't be measured directly for a real indentation test, because the thermocouple can never be placed right at the contact point. Other non-contact temperature measurement methods exist, such as Raman spectroscopy or infrared thermography, but these require additional input parameters that are hard to determine and so can cause big errors in the measured temperature. For this reason (and cost) they are not used in most currently high temperature IIT systems [11,12].

There is, therefore, a need for improved, calibrated methods to obtain valid temperature data in elevated temperature IIT. This paper investigates the limitation of using the measured thermal drift rate as an indicator for isothermal contact. Instead, an alternative practical method is proposed and step by step guidance given to establish an isothermal contact at a known temperature including the detection of the thermal equilibrium.

2. Experimental details

A Micro Materials platform three NanoTest indentation system (Wrexham, UK), extensively described elsewhere [13], was used in combination with their 'third generation' hot stage as shown in Figure 1. Briefly, the NanoTest system is a horizontal force application indentation testing device. The indenter and the sample can be heated to a set temperature separately with the aid of heating elements instrumented with Eurotherm controllers. There are two methods available to control this process: proportional-integral-differential (PID) control of a constant temperature, or a constant power input control. An aluminium heat shield is placed between the indenter and the pendulum to protect the back of the instrument and its sensors from direct radiant heating. The unique design of the 'third generation' hot stage outperforms older versions by providing an improved thermal isolation from the rest of the system. This includes a ceramic shroud that, when closed, further reduces the heat transfer from the hot zone into the rest of the instrument. This shroud also reduces convection currents, enhancing both thermal and mechanical stability of the instrument.

A Berkovich diamond indenter was used in this study. Indentations were carried out at temperatures up to 300°C on a copper sample and an advanced technical ceramic sample (NPL ID: JGG007) being developed at NPL as a high temperature reference material due to its high mechanical stability over temperature. The thermal conductivity of copper is approximately 400 $W \cdot m^{-1} \cdot K^{-1}$; while that of JGG007 is approximately 30 $W \cdot m^{-1} \cdot K^{-1}$. Both samples had dimensions of 20 mm x 20 mm x 3.6 mm and their surfaces were mechanically polished to a mirror finish. The samples were secured to the hot stage using a silicon dioxide based cement (Omega 600, Omega engineering) with a thermal conductivity in the range 1.44-1.73 $W \cdot m^{-1} \cdot K^{-1}$. The same cement was also used to mount a *k*-type thermocouple into a shallow groove machined in the surface of JGG007. For the copper sample, a *k*-type thermocouple was brazed to its surface with silver solder to provide a high thermal conductivity contact. In order to understand the process completely, the indenter and sample temperature histories were recorded throughout the entire nano-indentation experiment.

The following procedure was adopted for indentations at elevated temperatures: the sample and the indenter were separately heated to their set temperatures under PID feedback control, and left to stabilise with a distance of 50 µm between the indenter and the sample. The control loop of the indenter was then switched to constant power control at the power level required to maintain the set indenter temperature. The indenter and the sample were then moved to the normal indentation contact. A maximum indentation force of 100 mN was applied with a force application/removal time of 30 seconds. The dwell time at maximum force varied from 30 to 300 seconds. A 60 second hold segment was added to the pre-indentation (when the contact just occurs) and the post-indentation (at 10% of the maximum load) to allow the calculation of thermal drift rates.

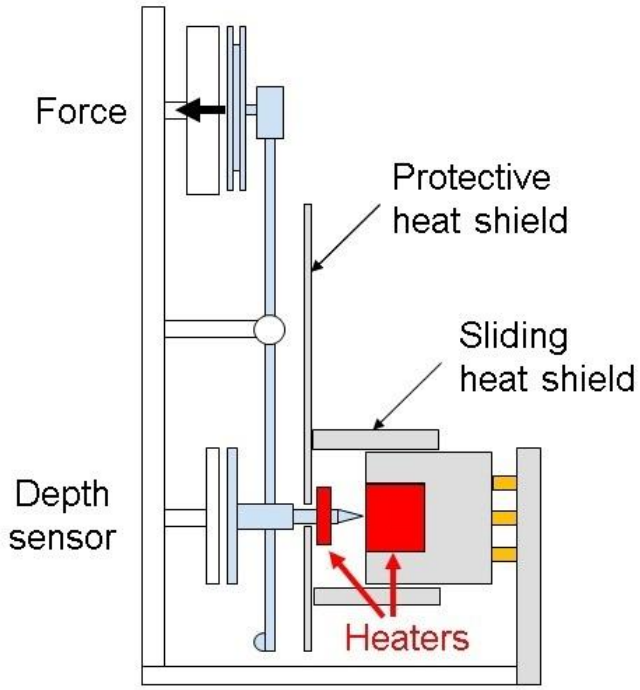

Figure 1 Schematic of a NanoTest system setup: the indenter and sample have separate heating elements with thermocouples linked to Eurotherm controllers to achieve the set temperatures. The heat shield provides thermal isolation of the hot zone from the body of the stage and the electronics behind the indenter.

3. Experimental results and discussion

3.1 Indenter temperature profile

A typical indenter temperature profile of a completed indentation experiment on the ceramic sample (JGG007) is shown in Figure 2 where the temperature of the indenter, as measured by its controlling thermocouple under constant power control, is recorded and plotted (left hand axis) as a function of the experiment time. The indenter tip is ideal for this due to its low thermal mass and high thermal conductivity. The depth sensor raw signal in volts (plotted in red with scale on the right hand Y axis) is superimposed on the temperature profile (plotted in blue with scale on the left hand Y axis). The depth sensor raw voltage signal may be converted to indentation displacement if a calibration value is applied. For the purpose of this paper, only the raw depth voltage signal is shown as this is sufficient to demonstrate the relative movement between the indenter and sample.

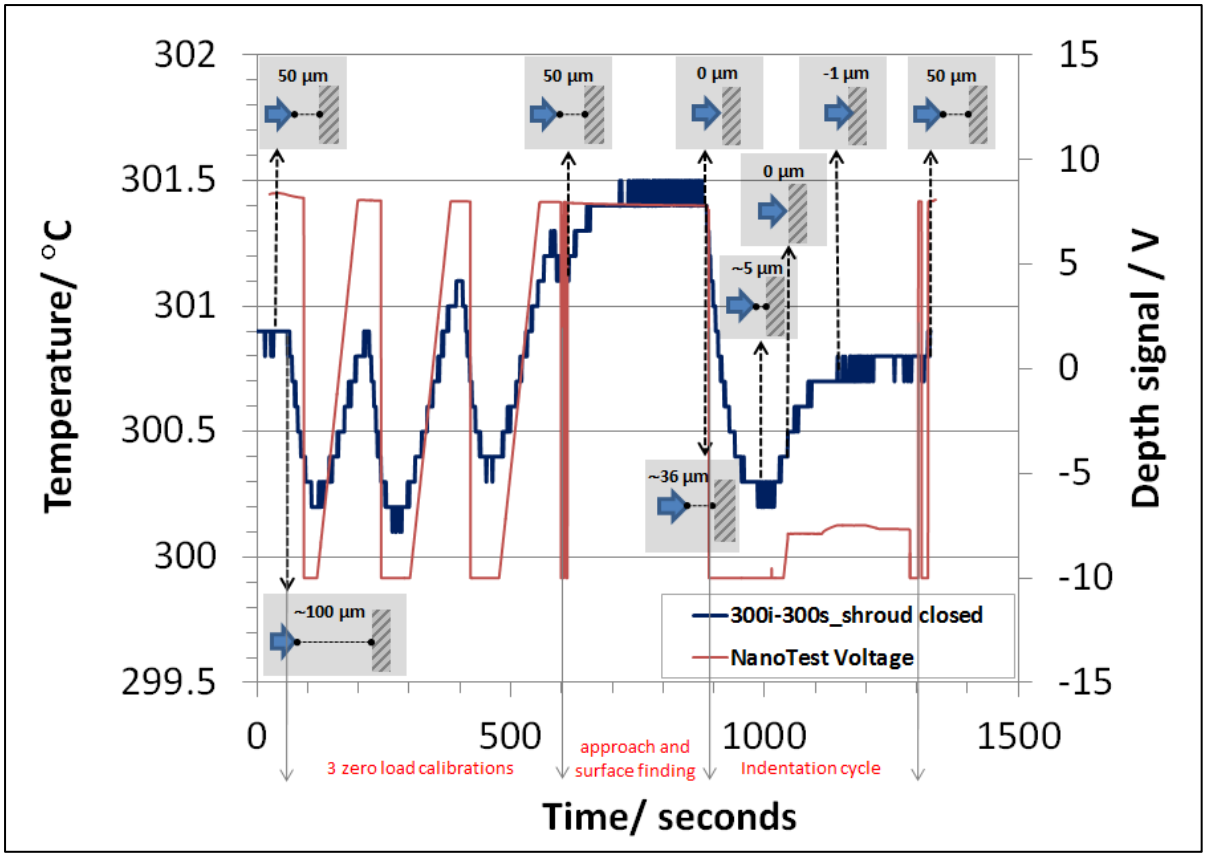

Figure 2 Indenter temperature profile (blue) as a function of indentation time from the beginning of an experiment on the ceramic sample (JGG007). The diamond indenter was heated under fixed-power control and the ceramic sample was heated under PID control. The indenter and sample were both set to a nominal temperature of 300 °C. The depth sensor raw signal in volts (red) is superimposed on the temperature profile and scaled according to the right hand side vertical axis.

At the beginning of an indentation experiment, the indenter and the sample were heated to 300 °C for a preliminary holding period of 60 seconds, with a separation of 50 µm; the sample heater was under PID control while the indenter heater was under fixed-power control. This is shown in Figure 2 as an initial plateau period, which indicates an initial thermal equilibrium. Before the sample started to move towards the indenter, three “zero-load calibrations” were performed, a unique feature of the NanoTest system cycle, during which it determines the small coil current required to bring the pendulum to its vertical, mechanical equilibrium position. The zero load calibration involves the movement of pendulum over a distance of around 50 µm (from -10.5V to ≈ 9V), this movement clearly disturbed the initial thermal stability by as much as 1°C in this particular setup. Figure 2 shows the three cycles of temperature fluctuations one for each of the zero load calibrations. It is interesting to notice that the indenter temperature increased slightly after each zero-load calibration cycle. This

may be due to the fact that the indenter requires a slightly longer cooling time than is allowed between zero force calibrations. After this, the sample was brought into contact with the indenter to detect the sample surface position while the indenter stayed at the stop point (≈ 9V); during this approach and surface finding period, the sample travelled (at a speed of 0.35 μm/second) towards the indenter and this process caused the indenter temperature to rise by 0.4 °C, which we will call the "proximity effect". Once the sample surface was detected, the indentation cycle started by moving back to the furthest position of the pendulum (-10.5V) to allow the sample to be moved into the preferred indentation position (-8V). When the sample is in position for indentation, the indenter was brought into contact with the sample (at a slower speed of 0.22 μm / second) in order to start a loading cycle and a temperature increase of 0.5°C was observed during this period. It is clearly seen that when the gap between the indenter and the sample was reduced, the indenter temperature increased; conversely, when the gap was increased the indenter temperature dropped. Both are due to the change in the net radiation received by the indenter as well as the convection currents between the indenter and sample when the distance between them changes. The indenter temperature profile is a useful tool to access these temperature fluctuations and to give guidance to configure the IIT system better (such as the position of the heat shield, the indenter and sample mounting, etc).

3.2 Quantification of the effect of heat transfer during indenter approach

The 'proximity effect' describes only one aspect of the rather complicated thermal situation when conducting an indentation at elevated temperatures. Figure 3 illustrates an overview of the temperatures present in the "hot zone" enclosed between the protective heat shield and ceramic shroud, including the indenter, the sample, and the thermocouples. In Figure 3(a), the sample and the indenter are separated and, in Figure 3(b), they are shown brought into contact. Different thermal configurations and their possible thermal outcomes are summarized in Table 1. In all cases, the indenter is heated under fixed-power control and the sample is heated under PID control and allowed to reach a thermal equilibrium.

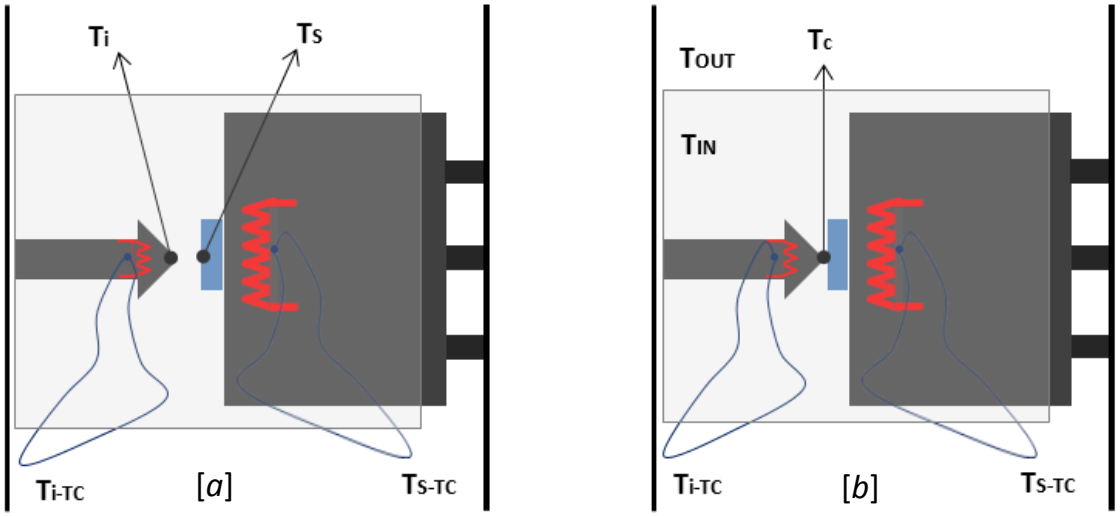

Figure 3 Basic elements of the Micro Materials hot stage including a ceramic shield, in closed position, thermally isolating the indenter and the sample from the cabinet environment: (a) the indenter and the sample are heated independently prior to contact; (b) the indenter and sample are brought into contact. The temperatures at different positions are recorded: $T_{i\text{-}TC}$ and $T_{S\text{-}TC}$ are the temperatures of control thermocouples for indenter and sample respectively; T_i and T_S are actual indenter tip and sample surface temperatures respectively; T_{IN} and T_{OUT} are the temperatures inside and outside the ceramic shroud respectively; T_C is the temperature of the contact point when indentation occurs.

In the ideal case of a perfectly isothermal hot zone, all the temperatures everywhere are the same (Table 1: case 1), i.e. the hot zone temperature (T_{IN}) is equal to the sample surface temperature (T_S) and the indenter tip temperature (T_I); thus no heat transfer will occur during the approach or the indentation cycle. In reality, although a ceramic shroud is used as a thermal barrier, there is always a heat loss from the enclosed hot zone into the instrument environment, which is consequently slightly elevated but typically maintained near room temperature. The temperature of the instrument environment outside the shroud (T_{OUT}) is, therefore, always lower than the hot zone inside the shroud (T_{IN}) and, for passively shielded hot zones, T_{IN} is always lower than the temperatures of the indenter tip (T_I) and sample surface to be contacted (T_S). In addition, in a real indentation test, the thermocouples can never be exactly placed at the indenter tip or at the position on the sample surface to be contacted; and the thermal gradient along each wire of the thermocouple (which determines the thermocouple output voltage) is not the same. Typically, control thermocouples are located behind the tip and the sample surface as shown in Figure 3. Therefore, there is always

a discrepancy between the thermocouple readings ($T_{I\text{-}TC}$ and $T_{S\text{-}TC}$) and the temperatures of the respective points of interest (T_I and T_S).

Table 1: Summary of possible configurations of indenter tip temperature (T_I), sample surface temperature (T_S) and their adjacent environment temperature (T_{IN}).

Case number	Prior to approach	T_I during approach	Possible combinations of T_I & T_S just before contact occurs	ΔT_I after contact occurs	Iso-thermal contact
#1	$T_I = T_S = T_{IN}$	0	$T_I = T_S$	0	√
#2	$T_S > T_I > T_{IN}$	↑	$T_S > T_I$	↑	×
#3	**$T_S > T_I > T_{IN}$**	**↑**	**$T_S = T_I$**	**0**	**√**
#4	$T_S > T_I > T_{IN}$	↑	$T_S < T_I$	↓	×
#5	$T_I > T_S > T_{IN}$	↑	$T_S < T_I$	↓	×
#6	$T_I > T_S > T_{IN}$	0	$T_S < T_I$	↓	×
#7	$T_I > T_S > T_{IN}$	↓	$T_S < T_I$	↓	×

When the distance between the indenter and the sample is reduced, as happens when they are brought toward contact, their thermal equilibrium is inevitably disturbed. The heat exchange between the indenter and sample and their adjacent environments changes with relative position. Since T_{IN} is always lower than T_I and T_S, reducing the separation between indenter and sample will increase the heat flux into both. Both temperatures will, therefore, tend to rise, but by different amounts depending on the thermal mass involved. Upon contact, the surface and tip temperatures will be forced to be the same, but any difference will result in a thermal gradient and a heat flow between sample and tip. This heat flow will be detected by the small thermal mass tip changing temperature due to the net power input to it changing. Various scenarios are possible as summarized in Table 1. Apart from a perfectly isothermal hot zone (case 1), there is only one possibility (case 3) that achieves an isothermal contact in thermal equilibrium at a known temperature. In this particular case, the indenter is set to a temperature just sufficiently below that of the sample surface as to be heated on approach so that it reaches the temperature of the surface exactly as it contacts. Calibration of the temperature difference between T_I and $T_{I\text{-}TC}$ at this condition of isothermal contact in thermal equilibrium then allows assignment of a calibrated value to the contact temperature, T_C. In

this way, an isothermal contact at a known temperature in thermal equilibrium can be achieved.

3.3 Calibration of the absolute indenter tip temperature

In practice, different samples will have different thermal conductivities. When changing samples, the mounting cement thickness is also likely to be different; T_S can, therefore, not be predicated from $T_{S\text{-}TC}$. The indenter, however, is essentially unchanged in geometry and materials from one experiment to the next. The only possible change that might cause a change in thermal conductivity of an indenter is a change in thermal contact with the mounting screws when the indenter is removed/replaced. The calibration of temperature difference between T_I and $T_{I\text{-}TC}$ is the best chance of obtaining a known and reproducible temperature at the contact point. A calibration method is, therefore, required that can determine T_I, T_C & T_S and demonstrate that T_S=T_C=T_I at contact. The temperature offset between T_I and $T_{I\text{-}TC}$ can then be determined by knowing T_C. This is achieved by studying the indenter temperature profile when indenting into a thermocouple junction, a similar approach as described in [14]. A sample with a high thermal conductivity was used, in this case copper, to maximise the conductive heat flux on contact for any temperature difference between tip and surface and to minimise any temperature gradients in the sample surface. A *k*-type thermocouple was brazed to the sample surface with silver solder. The thermocouple reading ($T_{J\text{-}TC}$) was considered to be the best estimate of T_C when the indenter is in contact. A similar indentation cycle as described in section 3.1 was used. The proximity effect was studied by slowly approaching the sample towards the indenter at specific steps (50 µm, 25 µm, 15 µm, 5 µm and 0 µm) and resting in those positions for periods of 300 seconds. $T_{I\text{-}TC}$ was deliberately varied around three set sample temperatures ($T_{S\text{-}TC}$ set to be 100°C, 200°C or 300°C) in order to cover the temperature range within which T_I could be found to match T_S; upon a match T_I was assigned to be $T_{J\text{-}TC}$. It is important that the calibration values are obtained when the tip is in isothermal thermal equilibrium contact with the sample. Only in this condition can the heat flux balance (and so the temperature difference between tip and thermocouple) be the same as for a subsequent measurements at the same temperature.

An example of the indenter temperature profile during approach is shown in Figure 4, when $T_{I\text{-}TC}$ and $T_{S\text{-}TC}$ were set to be 255°C and 300°C respectively. The proximity effect is clearly

demonstrated; the 300 seconds pause at each step gives a better chance to reach thermal equilibrium before the next movement (this was only necessary to quantify the proximity effect). The rate of the indenter temperature increase drops as the indenter gets close to the sample surface because the rate of change in heat flux is proportionally reduced. During approach, the indenter temperature increased by as much as 1°C due to the change in heat transfer between the sample and indenter (believed to be mainly radiative). A similar temperature profile from the sample side can also be obtained by the reading from T_{JC}, but it was found that the temperature increase was less (only 0.5°C) due to the bigger thermal mass and high thermal conductivity of the sample assembly and the response of the sample heater PID control.

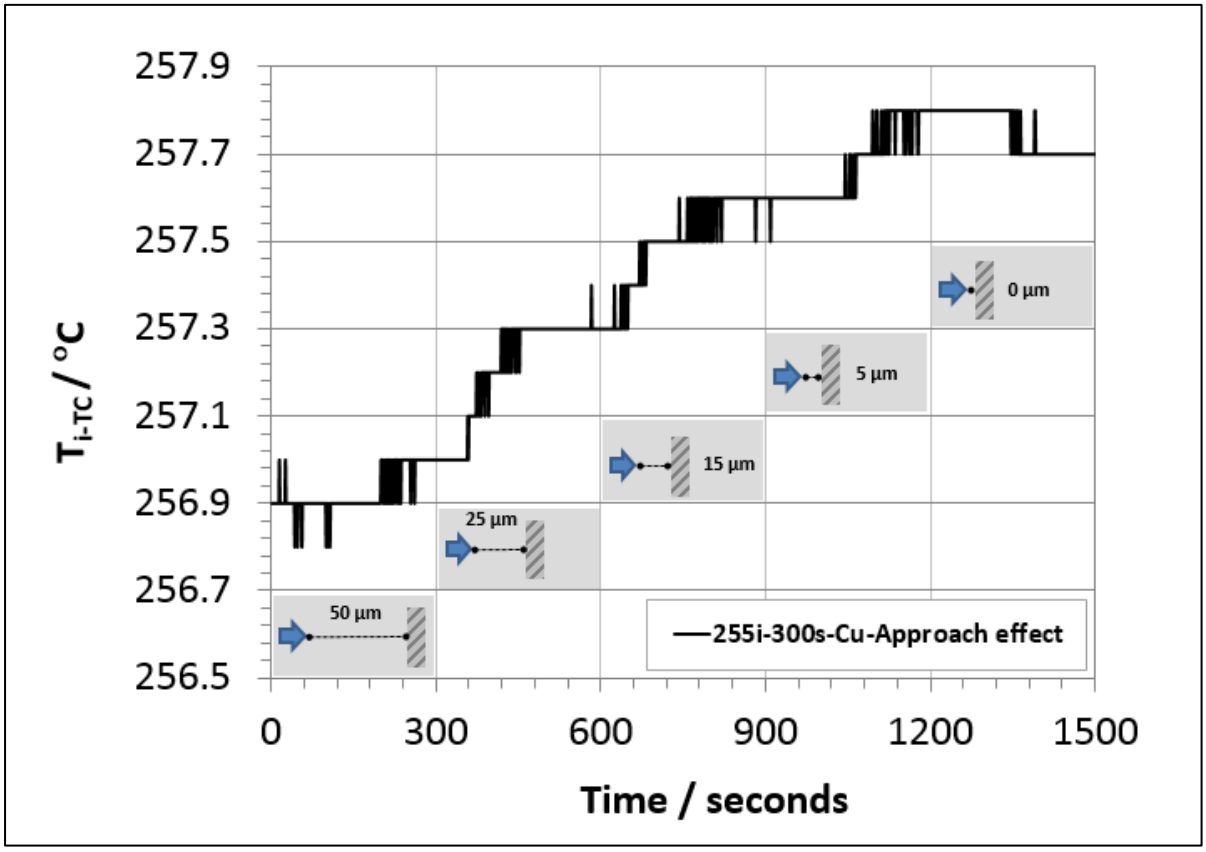

Figure 4 The proximity effect: the indenter temperature is plotted again the time elapsed from the beginning of the test. The sample is heated to a nominal 300°C and the indenter was heated to a nominal 255°C.

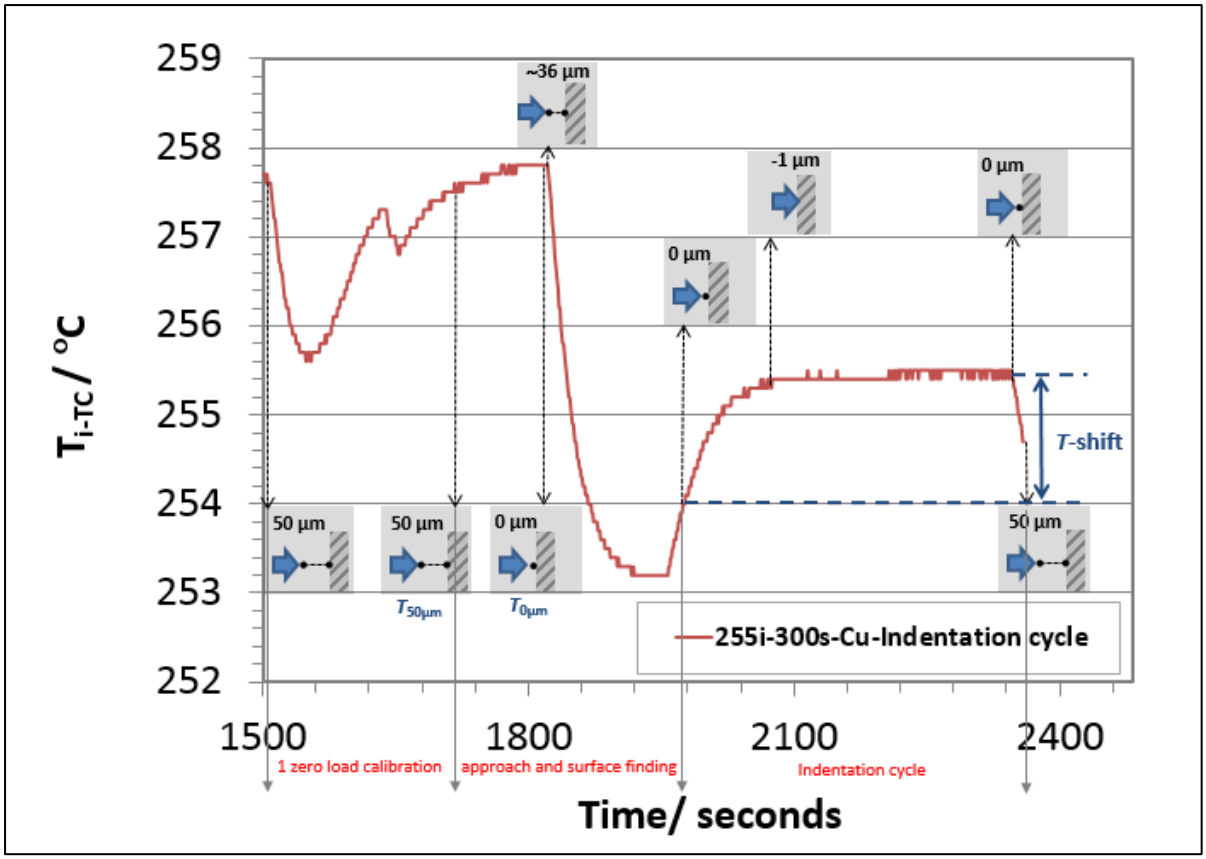

Figure 5 The indenter temperature profile during the indentation cycle on copper: the indenter nominal temperature was set to be 255°C and the copper sample nominal temperature was set to be 300°C.

The indenter temperature profile in Figure 5 shows the indenter temperature variation throughout the whole indentation experiment. In order to find the most sensitive way to describe the temperature mismatch between $T_{I\text{-}TC}$ and $T_{S\text{-}TC}$ (for this particular case, $T_{I\text{-}TC}$= 255°C and $T_{S\text{-}TC}$=300°C), the temperatures at different positions were investigated and compared with that at contact: $T_{5\mu m}$ is used to represent the indenter temperature when it is 5µm away from the sample surface during approach; $T_{0\mu m}$ is defined as the indenter temperature when contact occurs; e.g. T_{shift} = $T_{0\mu m}$ - $T_{5\mu m}$ is the indenter temperature shift during the final approach. The "T_{shift} during the experiment cycle" is defined as the indenter temperature difference experienced between the initial contact point and the maximum penetration depth point (as shown at far right hand side of Figure 5). These temperature values were obtained for all $T_{I\text{-}TC}$ and $T_{S\text{-}TC}$ combinations investigated and are summarized in Figure 6. The temperature shift results all have a similar trend: when the same sample nominal temperature was kept constant at the set point ($T_{S\text{-}TC}$ =100°C, 200°C or 300°C), T_{shift} on contact went from positive to negative as $T_{I\text{-}TC}$ increased. As T_I goes from below T_S (colder

than the sample surface) to above T_S (hotter than the sample surface), the heat gained by the indenter gradually reduces and eventually the indenter actually cools as it approaches the sample (presumably $T_I > T_S$). The temperature at which T_{shift} is zero is the best estimate of when isothermal contact occurs (shown in Figure 6 as the intercept point between the linear fitting line and horizontal line when $\Delta T=0$) and, at this point, the $T_{J\text{-}TC}$ was assigned as the true contact temperature, T_C. Note that the sensitivity of the indenter to a temperature difference between tip and surface at contact is proportional to the time allowed for thermal equilibrium to be reached post-contact. In this study, the "T_{shift} during the experiment cycle" was chosen as the representative parameter defining the isothermal contact, because it is a more sensitive parameter and it reflects whether the temperature was stable throughout contact, which is the practical requirement for an iso-thermal contact in thermal equilibrium in a real experiment.

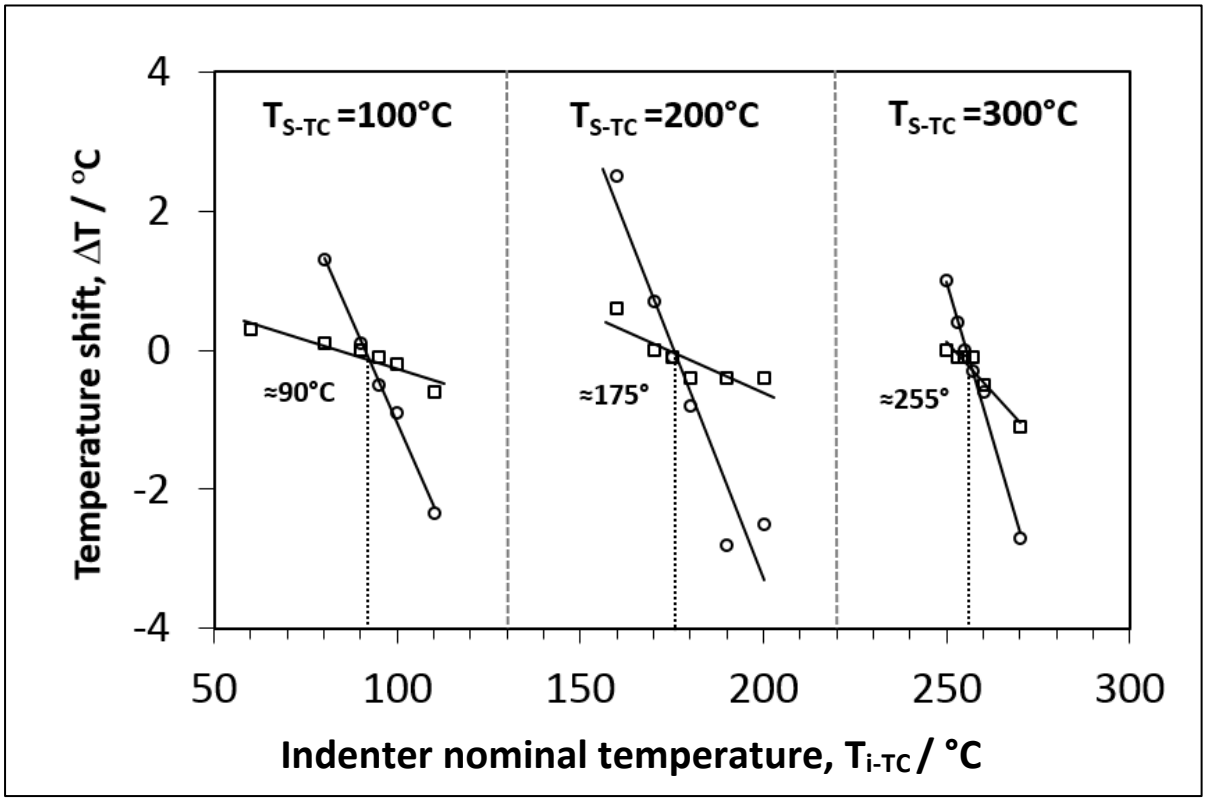

Figure 6 Indenter temperature shifts as a function of the temperature combination of the indenter and the copper sample nominal temperature, $T_{I\text{-}TC}$ and $T_{S\text{-}TC}$ respectively. The open squares are for temperature shift between 0->5 μm and the open circles are for the for temperature shift during the experiment cycles.

A calibration of the absolute indenter tip temperature with respect to the control thermocouple reading was then obtained by comparing the $T_{I\text{-}TC}$ and $T_I = T_{J\text{-}TC}$ as shown in

Figure 7. A linear function was found to be a good fit to the three calibration points obtained. It is important to point out that this calibration is increasingly important as the contact temperature increases. Strictly, the calibration is only exactly valid for the specific tip-sample configuration used for the calibration experiments. The exact temperature difference between tip and thermocouple will be affected by parameters that can alter the heat transfer mechanisms (i.e. the screwing torque of the indenter mount, the position of the heat shield, the sample emissivity, etc.). Thus, consideration should be given as to what extent such changes may affect the calibration and whether it is still valid. It is recommended that the calibration be revalidated whenever the indenter is changed or re-mounted. When this method is used, there appears to be little benefit from putting the sample controlling thermocouple T_{SC} on the sample surface. Although this will certainly make the thermal loop shorter it makes no difference to the indenter tip temperature calibration. The highest uncertainty in temperature measurement occurs for samples with low thermal conductivity, where large thermal gradients are easily established. A surface thermocouple can help with control, but needs to be shielded from the tip heater to prevent it being strongly heated by radiant energy from the indenter; causing significant PID errors.

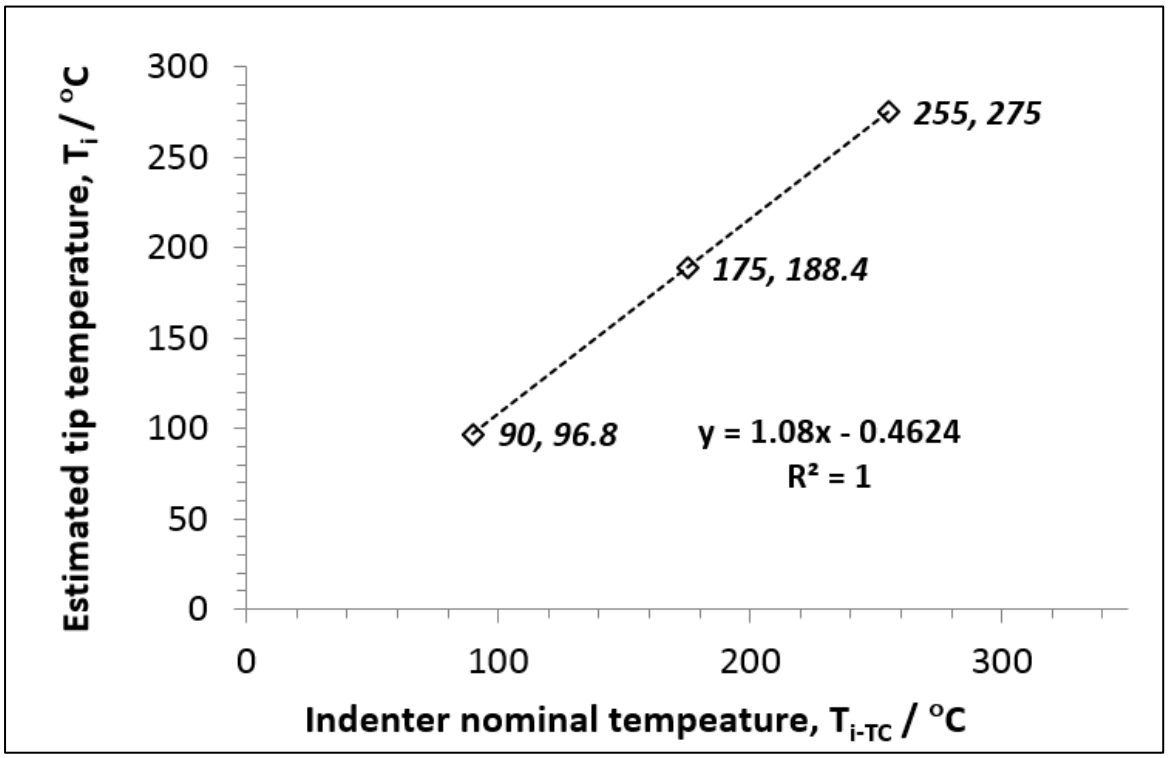

Figure 7 Calibration of the absolute indenter tip temperature: the estimated actual tip temperature T_I as a function of the nominal tip temperature $T_{I\text{-}TC}$.

3.3 Thermal drift rate and isothermal contact under thermal equilibrium

During the absolute indenter tip temperature calibration in section 3.2, the calibration indentation cycle included a 60 seconds hold segment (pre and post indentation as described in Section 2) so that the thermal drift rate could be calculated and compared to the isothermal equilibrium contact temperature. Thermal drift rates are plotted in Figure 8 and clearly show a correlation between the size of temperature difference (between the indenter and the sample on contact), and a higher thermal drift rate. In most cases, the thermal drift is negative when the indenter is colder than the sample and becomes positive as the temperatures difference reduces. This suggests that tip and sample thermal expansion on a local-scale can be a significant contributor to the overall measured drift rate. When the indenter is colder than the sample, it acquires heat during contact and expands causing negative drift; conversely, a hotter indenter will contract upon contact, giving a positive thermal drift. The opposite effect will happen to the sample, which will go a little way towards compensating the indenter expansion or contraction. The effect on the sample depends on its thermal expansion coefficient and on the temperature gradient in the sample near the contact, which depends on its thermal conductivity. The combined behaviour between indenter and sample will contribute to the overall measured thermal drift, which is also affected by changes in heat input to the instrument environment (e.g. when the hot zone temperature is changed) that may happen on a different time scale. This is thought to be the cause of the large scatter in measured thermal drift rates, as the 300°C case demonstrates in Figure 8. Based on these results, we show that the new method we demonstrate here is a significantly more accurate method of determining iso-thermal contact in thermal equilibrium and assigning a valid temperature than the current methods using thermal drift, which can easily cause an error of a several degrees. The scattering of the thermal drift rate data makes the thermal drift method even less reliable. Generally speaking, it is always a big challenge to separate the thermal drift rate from the indentation creep into the test piece for instrumented indentation testing. This is a well-known and common problem when indenting soft materials such as polymers at room temperatures. When conducting indentation tests at elevated temperatures, most materials (not only polymers) will become softer and creep more under the same loading condition; as a result, it becomes even more difficult to obtain a reasonable

estimation of the true thermal drift rate due to the more significant indentation creep, especially for inhomogeneous materials.

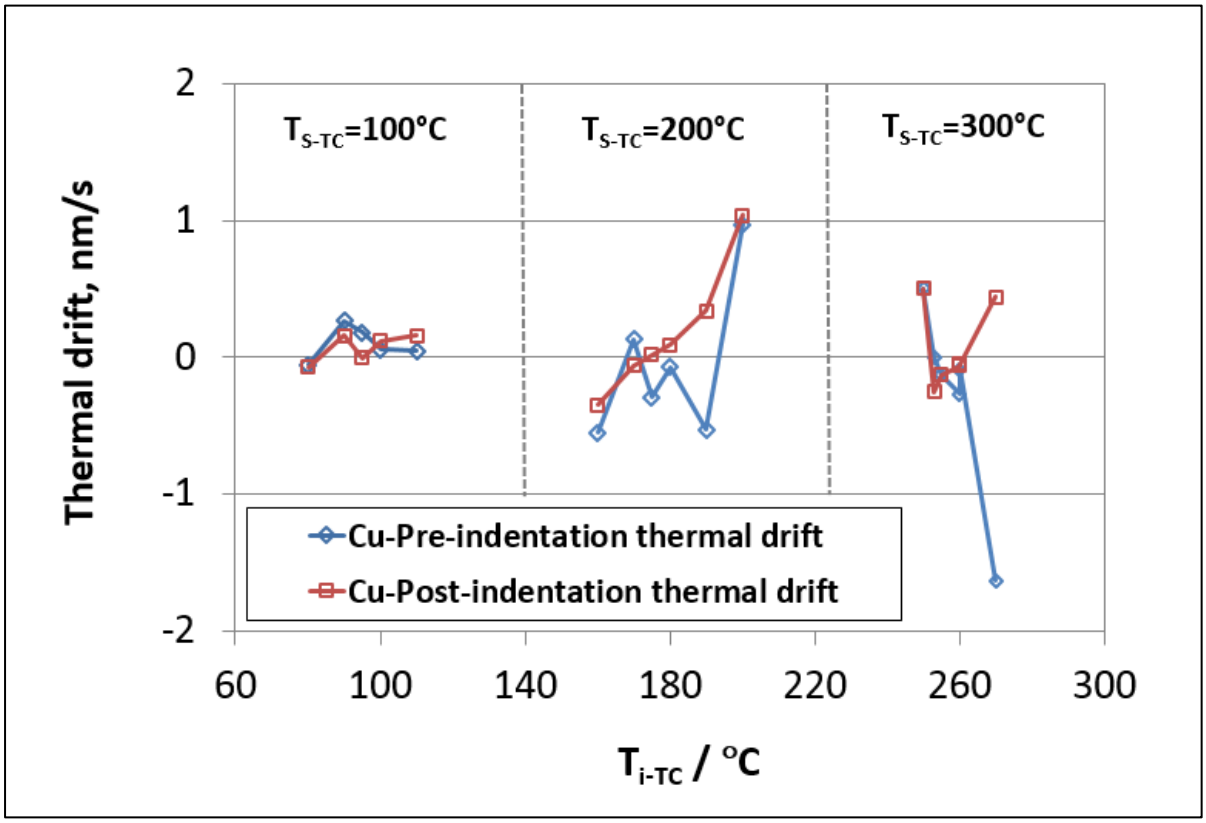

Figure 8 The calculated pre- and post-indentation thermal drifts at various indenter and sample temperature combinations.

4. Summary

We have demonstrated a practical method to achieve an isothermal contact at a known temperature in thermal equilibrium for IIT systems capable of heating the sample and indenter independently. This method is much more sensitive and accurate than methods using the measured thermal drift rate as an indicator of isothermal contact, which are shown may lead to large errors in estimating the real contact temperature.

The new method uses the indenter temperature profile during an indentation as a sensitive and unique signature of the system thermal setup. A high thermal conductivity sample and a calibrated thermocouple have been used to calibrate the temperature difference between

indenter tip real temperature (T_I) and nominal indenter temperature given by the control thermocouple reading ($T_{I\text{-}TC}$). This difference was found to be as large as tens of degrees.

Finally, a step by step guidance is recommended for establishing isothermal contact at a known temperature under thermal equilibrium in elevated temperature instrumented indentation testing:

- Step 0: obtain the absolute indenter tip temperature calibration by indenting into a thermocouple junction mounted on a sample of high thermal conductivity heated to be in isothermal thermal equilibrium with the indenter tip, i.e. calibrate the temperature difference between T_I and $T_{I\text{-}TC}$ in a similar thermal environment to that of future measurements. It is recommended also to note the typical offset between the sample heater thermocouple reading and the measured T_I to assist with future sample heater set up.
- Step 1: set the sample heater PID control to target the required value of T_C allowing for the estimated offset between T_S and $T_{S\text{-}TC}$.
- Step 2: Use the calibrated offset between T_I and $T_{I\text{-}TC}$ to set the indenter PID control to target the required T_C and when this temperature is reached then switch to fixed-power control to maintain that temperature.
- Step 3: bring the sample and indenter to close proximity
- Step 4 (optional): Using previous experience of the proximity effect to adjust the indenter heating power and or sample heater to obtain values of T_I and T_S likely to achieve the target temperature T_C at contact.
- Step 5: approach to contact and hold for at least 60 seconds. Monitor $T_{I\text{-}TC}$ through the process. If $T_{I\text{-}TC}$ changes, unapproach, readjust indenter power or sample heater set point and (after reaching thermal equilibrium) approach again; repeat until $T_{I\text{-}TC}$ doesn't change on contact. Note that the sensitivity of $T_{I\text{-}TC}$ to tip-sample temperature difference reduces as sample thermal conductivity reduces. In such cases, the best approach may be to use step 4.
- Step 6: conduct the indentation loading cycles as required. The contact temperature T_C is given by looking up the indenter tip calibration function using the known $T_{I\text{-}TC}$ reading.

Acknowledgement

The authors acknowledge collaboration with Micro Materials Ltd., who provided expertise and instrumentation for this work. We acknowledge the funding of the EMRP. The EMRP is jointly funded by the EMRP participating countries within EURAMET and the European Union.

References

[1] Smith J F and Zheng S 2000 High temperature nanoscale mechanical property measurements *Surf. Eng.* **16** 143-146

[2] Maxwell A S, Monclus M A, Jennett N M and Dean G 2011 Accelerated testing of creep in polymeric materials using nanoindentation *Polym. Test.* **30** 366-371

[3] Schuh C A, Packard C E and Lund A C 2006 Nanoindentation and contact-mode imaging at high temperatures *J. Mater. Res.* **21** 725-736

[4] Trenkle J C, Packard C E and Schuh C A 2010 Hot nanoindentation in inert environments *Rev. Sci. Instrum.* **81** 073901

[5] Huang X, Nohava J, Zhang B and Ramirez A G 2011 Nanoindentation of NiTi shape memory thin films at elevated temperatures *International Journal of Smart and Nanomaterials* **2** 39-49

[6] Wheeler J M, Raghavan R and Michler J 2011 In situ SEM indentation of a Zr-based bulk metallic glass at elevated temperatures *J, Mater. Sci. Eng. A* **528** 8750-8756

[7] Gibson J S K-L, Roberts S G and Armstrong D E J 2015 High temperature indentation of helium-implanted tungsten *Mater. Sci. Eng. A* **625** 380-384

[8] BS EN ISO 14577-1:2002, ISO 14577 metallic materials – Instrumented indentation test for hardness and materials parameters, BSI, London, 2002. ISBN 0 580 40792 6.

[9] Wheeler J M and Michler J 2013 Invited Article: Indenter materials for high temperature nanoindentation *Rev. Sci. Instrum.* **84** 101301

[10] Everitt N M, Davis M I and Smith J F 2011, High temperature nanoindentation – the importance of isothermal contact *Phil. Mag. A* **91** 1221-1244

[11] Wheeler J M, Armstrong D E J, Heinz W and Schwaiger R 2015 High temperature nanoindentation: The state of the art and future challenges *Curr. Opin. Solid State Mater. Sci.* **19** 354-366

[12] Wheeler J M, Brodard P and Michler J 2012 Elevated temperature, in situ indentation with calibrated contact temperatures *Phil. Mag. A* **92** 3128-3141

[13] Jennett N M and Nunn J 2011 High resolution measurement of dynamic (nano) indentation impact energy: a step towards the determination of indentation fracture resistance *Phil. Mag.* **91** 1200-1220